Progress in Oceanography xxx (xxxx) xxx–xxx

Contents lists available at ScienceDirect

Progress in Oceanography

journal homepage: www.elsevier.com/locate/pocean

Seasonal organic matter dynamics in a temperate shelf sea

Clare E. Davis[a,*], Sabena Blackbird[a], George Wolff[a], Malcolm Woodward[b], Claire Mahaffey[a]

[a] Department of Earth, Ocean and Ecological Sciences, University of Liverpool, 4 Brownlow Street, Liverpool L69 3GP, UK
[b] Plymouth Marine Laboratory, Prospect Place, Plymouth PL1 3DH, UK

ARTICLE INFO

Keywords:
Organic matter
Continental shelf
Carbon export

ABSTRACT

Organic matter (OM) plays an important role in productive shelf seas and their contribution to global carbon (C) and nutrient cycles. We investigated dissolved and particulate OM (DOM and POM, respectively) dynamics over a seasonal cycle in the Celtic Sea. The quantity of OC was largest during the spring bloom and lowest in autumn. DOM was always C rich relative to the POM pool and the Redfield ratio (106C:16N:P). There was clear decoupling between C, N and P and the response of OM composition to different seasons and nutrient statuses of the microbial community. The C:P stoichiometry was much more variable than the C:N stoichiometry, which was near constant. Downward OC fluxes were dominated by POM during bloom events and DOM during the stratified summer. In terms of partitioning, 92–96% of OC was in the DOM pool throughout sampling, which given its high C:N (12.4–17) suggests it was an efficient vehicle for potential off-shelf export of C during winter mixing.

1. Introduction

Organic matter (OM) is a broad term applied to a large group of carbon containing molecules that are produced throughout the food web. It is operationally defined as either dissolved (DOM, i.e. that passing through a 0.7 μm filter) or particulate (POM, i.e. that retained on the filter). It is comprised of carbon (C), nitrogen (N) and phosphorus (P) and other elements and includes compounds such as carbohydrates, amino acids and phospholipids (Benner, 2003). OM constitutes the largest bioactive C reservoir on Earth (Kepkay, 1994). This reservoir is dominated by the DOM pool, which has a typical C:N:P ratio of 300:25:1 and is an efficient potential export vehicle of organic C from surface water to the deep ocean (Hopkinson et al., 1997; Hopkinson and Vallino, 2005). Therefore, marine OM dynamics have a strong influence on both global nutrient cycles and atmospheric carbon dioxide.

There are allochthonous and autochthonous sources of OM in the marine environment. Allochthonous sources include river inputs, groundwater release, release from sediments and atmospheric deposition, in addition to a background refractory contribution. The principal autochthonous source of POM is *in situ* photosynthesis by phytoplankton, which in turn provides a source of DOM via extracellular release, grazer mediated release or excretion, and bacterial or viral cell lysis, amongst other processes. Sinks of OM include aggregation, sedimentation and burial, remineralisation by heterotrophic processes to its inorganic constituents (Azam et al., 1983), photodegradation (Moran and Zepp, 1997), ectoenzyme facilitated hydrolysis induced by nutrient-stressed microbes (e.g. Cembella et al., 1984), and utilisation as a food source for higher trophic levels. Thus, DOM production is inextricably coupled to POM dynamics.

The bioavailability of OM, its transfer through trophic levels and its fate are strongly influenced by chemical composition and molecular size class (Amon and Benner, 1996). OM is commonly classed as either labile (turnover times of minutes to days), semi-labile (weeks to years), or refractory (decades to millennia) (Ducklow, 2000). Lability is strongly governed by residence time and microbial processes (Azam et al., 1983). As such, older low molecular weight refractory OM is typically more C-rich relative to N and P than fresher high molecular weight labile OM (Amon and Benner, 1996). Lability and stoichiometry therefore affect the quality of OM and its potential as a source of C and energy for heterotrophs and as a nutrient source for autotrophs and higher trophic levels (Lønborg and Alvarez-Salgado, 2012). Stoichiometry of OM is also important in terms of C export efficiency, with deviations from Redfield influencing the magnitude of C export relative to N and P from the surface ocean (Hopkinson and Vallino, 2005; Barron and Duarte, 2015).

The elemental stoichiometry of the bulk OM pool is a combination of both living (e.g. phytoplankton biomass) and detrital material (e.g. faecal matter, detritus, humification products, complex geopolymers) (Hedges et al., 2001; Carlson and Hansell, 2014; De Leeuw and Largeau, 1993). Despite many transformations through the marine food web, it is common that the stoichiometry of autotrophic biomass plays an important role in setting the stoichiometry of the bulk POM pool and higher trophic levels (Sterner and Elser, 2002). Thus, bulk stoichiometry is influenced by factors affecting autotrophic biomass, such as

* Corresponding author.
E-mail address: davis@liverpool.ac.uk (C.E. Davis).

https://doi.org/10.1016/j.pocean.2018.02.021

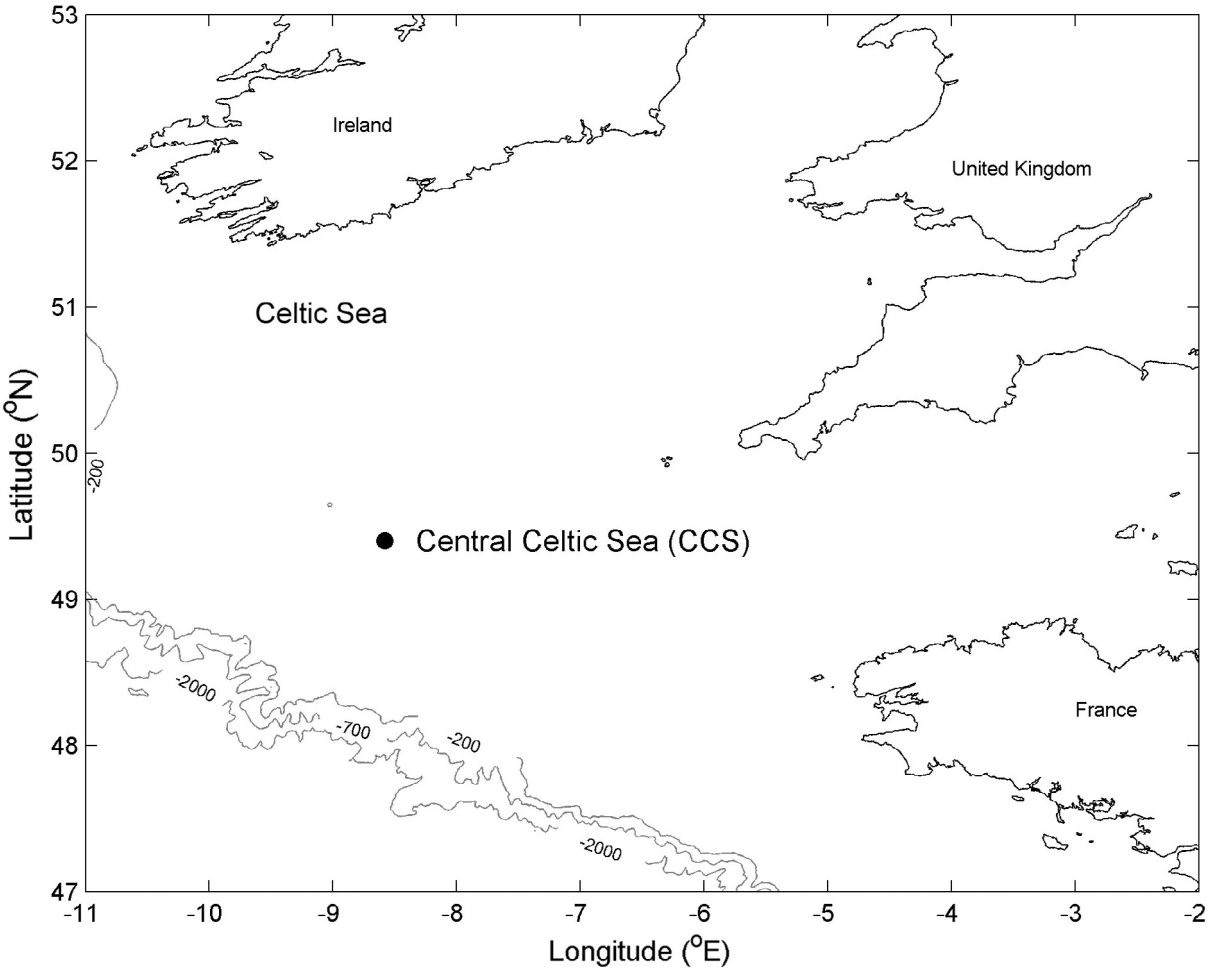

Fig. 1. Location of the Central Celtic Sea site (CCS) in the Celtic Sea, NW European shelf, adapted from Carr et al. (this issue).

inorganic nutrient availability, light, growth stage, community composition (Sterner and Elser, 2002; Arrigo, 2005; Klausmeier et al., 2008), as well as age/residence time and the degree of heterotrophic degradation and remineralisation (Sterner and Elser, 2002; Arrigo, 2005).

DOM is more C rich than POM due to its involvement in the microbial loop and C overproduction by phytoplankton (Carlson et al., 1998; Jiao et al., 2010). The longer OM is exposed to remineralisation, degradation and regeneration processes, the more its stoichiometry and lability are altered. DOM is produced through exudation by phytoplankton, cell lysis, sloppy feeding during zooplankton grazing on their prey, and solubilisation of POM (Carlson and Hansell, 2014). Refractory DOM is considered a sink of atmospheric CO_2 on timescales that are significant to climate models (> 50 years) and is thought to be generated through exudation associated with bacterial production, selective ecto-enzyme activity and via viral cell lysis, e.g. release of cell wall material (Jiao et al., 2010). The result is that the microbial carbon pump transfers proportionally more C to refractory OM that it does N and P, and this creates an efficient component of the C pump (Azam et al., 1983). Therefore, when assessing C export and the export efficiency of a system it is important to determine the relative contributions of both POM and DOM.

Shelf seas are highly dynamic and productive regions of the global ocean whose importance in global nutrient and carbon cycles is disproportionate to their size; contributing 15–30% of global primary production despite representing < 10% of the global ocean by area (Wollast, 1998). Simplistically, the continental shelf pump (CSP) can be viewed as a series of processes where firstly POM is produced in the euphotic zone via photosynthesis, which transfers inorganic C to the organic pool. Secondly, OM is transferred below the thermocline where it is remineralised to dissolved inorganic C (DIC) and is isolated from atmospheric exchange. And finally, to complete the export pathway this DIC must be advected off shelf to the adjacent open ocean. However, the CSP also includes riverine contributions and direct export of OM (Harrison et al., 2005). Like the open ocean, the efficiency of the CSP is reliant on the transfer of OM in excess of Redfield stoichiometry (i.e. C rich) below the thermocline and off shelf, allowing N and P regeneration and retention on shelf in the euphotic layer where they can support further production (Simpson and Sharples, 2012). Whether shelf seas are a net source or sink of CO_2 is dependent on the balance of autotrophic and heterotrophic processes, i.e. whether production of OM exceeds respiration of autochthonous and allochthonous OM (Tsunogai et al., 1999; Thomas et al., 2004). In some instances, shelf C dynamics are determined by ocean circulation, which affects the supply of deep ocean nutrients on shelf, while in other cases C dynamics are controlled by river inputs (Bauer et al., 2013).

The Shelf Sea Biogeochemistry programme consisted of an intense and wide-ranging sampling effort conducted in 2014 and 2015 to examine the CSP over a full seasonal cycle. Here, we present data from a series of cruises based in the Celtic Sea focussing on pelagic OM distributions and stoichiometry to improve our understanding of the role of OM in the CSP. These bulk OM dynamics are the result of a combination of factors including the stoichiometry of primary production, nutrient recycling, trophic transfer and decomposition which will vary across a seasonal cycle and inherently influence shelf-atmosphere-open-ocean C exchanges (Bauer et al., 2013). Our sampling campaign

included cruises in November 2014, March 2015, April 2015 and July 2015, selected to represent the breakdown of seasonal stratification, a mixed winter water column, the onset of seasonal stratification and the summertime stratified period, respectively. Repeat visits were made to specified sites within each cruise. Together, this allowed us to compare longer term seasonal variability and shorter-term variability, such as the spring-neap tidal cycle, and thus overall provide a better understanding of the contribution of OM to nutrient cycling in the Celtic Sea. We found decoupling of the dissolved and particulate organic pools as well as deviations in OM stoichiometry at key times of the year, thus results will be presented focussing on these features while addressing the following specific research questions: (a) how does the distribution and magnitude of organic C, N and P pools vary across a seasonal cycle in the Celtic Sea? (b) How does variable elemental stoichiometry in the Celtic Sea influence the CSP? (c) How does the role of sinking POM compare to that of DOM in the CSP?

2. Material and methods

Samples were collected on board the *RRS Discovery* (cruises DY018, DY021, DY029 and DY033) in the Celtic Sea located at CCS (central Celtic Sea, 49.4°N 8.5°W; Fig. 1). The cruises were selected to represent autumn (DY018, November 2014, $n = 3$), winter (DY021, March 2015, $n = 1$), spring (DY029, April 2015, $n = 5$), and summer (DY033, July 2015, $n = 4$). The sampling campaign (November 2014 to August 2015) consisted of measurements of vertical CTD profiles and sample collection for analysis of dissolved inorganic nutrients, chlorophyll *a* (hereafter Chl *a*), and dissolved and particulate organic nutrients.

2.1. Hydrography, chlorophyll a and dissolved inorganic nutrients

A rosette frame, supporting a Seabird 911 conductivity, temperature, depth (CTD) instrument, fluorometer and 20 L Niskin bottles was used to determine the vertical gradients in salinity, temperature and calibrated Chl *a* fluorescence, and collect seawater samples throughout the water column. Inorganic nutrients (dissolved inorganic nitrogen including ammonium, DIN; and phosphate, DIP) were collected directly from the CTD into aged, acid-washed and Milli-Q rinsed 60 mL HDPE Nalgene® bottles. Sampling, handling and analysis complied with recommendations in the International GO-SHIP nutrient manual (Hydes et al., 2010). Nutrients were analysed on board using a Bran and Luebbe segmented flow colorimetric auto-analyser using techniques described in Woodward and Rees (2001). Nutrient reference materials (KANSO, Japan) were analysed each day to check precision and accuracy. Precision was between 2% and 3%, with limits of detection of 0.02 μM for nitrate and phosphate, and 0.01 μM for nitrite.

2.2. Particulate organic matter (POM) sample collection

Particulate organic matter concentrations were determined at 6–8 depths through the water column with seawater samples collected from 20 L Niskin bottles mounted on a CTD/rosette frame.

In addition, during autumn, spring and summer cruises (DY018, DY029 and DY033) marine snow catchers (MSC), which are essentially large volume settling columns, were deployed both above and below the thermocline to segregate particles based on their sinking rate over a predetermined period (Cavan et al., 2015). Particle fractions defined as 'suspended' (POM_{susp}), 'slow sinking' (POM_{slow}) and 'fast sinking' (POM_{fast}) were sampled at the end of this settling period from the top of the MSC column, the lower MSC column, and the removal base tray of the MSC, respectively. Sampling the POM_{slow} fraction included a background of POM_{susp}, therefore this value was subtracted from POM_{slow} to estimate the contribution from slow sinking particles alone ($POM_{slow\text{-}susp}$). POM_{slow}, $POM_{slow\text{-}susp}$ and POM_{fast} concentrations were normalised to the original volume of the snow catcher to provide *in situ* concentrations as described in Davis and Mahaffey (2017). Standard deviations were derived for each particle fraction from repeat deployments during each cruise. The error associated with $POM_{slow\text{-}susp}$ was calculated according to Miller and Miller (2005):

$$SD_{slow-susp} = \sqrt{(SD_{susp}^2 \times SD_{slow}^2)} \div (n-1)$$

where SD_{susp} is the standard deviation derived from repeated sampling of POM_{susp}, SD_{slow} is the equivalent for POM_{slow}, and n is the number of repeat samples.

To determine particulate organic carbon and nitrogen (POC and PON) and particulate phosphorus (PPhos) content, measured volumes of seawater and marine snow catcher particle fractions were filtered onto Whatman glass fibre filter (GF/F, 25 mm diameter, 0.7 μm pore size, precombusted for 4 h at 450 °C for POC/PON, plus additional acid washing, deionized water rinsing and drying at 50 °C for PPhos) prior to storage at −20 °C until laboratory analysis.

2.3. POM analyses

All filters were freeze-dried prior to analysis. POC and PON were analysed in duplicate after vapour phase decarbonation using a Carlo Erba Instruments NC2500 elemental analyser (Yamamuro and Kayanne, 1995). A two-point calibration is performed using High Organic Sediment Standard OAS (Elemental Microanalysis Ltd, NIST certified values), which was then analysed twice as an unknown during the run. The results were always within the uncertainty limits of the certified value which are 7.17 ± 0.09% carbon and 0.57 ± 0.02% nitrogen, with detection limits of 100 ppm for both C and N.

PPhos was determined by dissolved inorganic phosphorus (DIP) analysis as in Davis et al. (2014), following high-temperature combustion and extraction in 5 mL of 0.5 M hydrochloric acid (Karl et al., 2001). PPhos was analysed in duplicate, and certified reference materials (SRM 1515 Apple Leaves, NIST) were analysed in triplicate with each sample extraction to ensure analytical precision and accuracy were within 2%. The limit of detection was 10 nM.

2.4. Dissolved organic matter (DOM) sample collection

Dissolved organic matter concentrations were determined at 6–8 depths through the water column with seawater samples collected from 20 L Niskin bottles mounted on a CTD/rosette frame. To determine dissolved organic carbon, total dissolved nitrogen and total dissolved phosphorus (DOC, TDN and TDP, respectively) concentrations, samples were filtered through Whatman glass fibre filter (GF/F, 47 mm diameter, 0.7 μm pore size, precombusted for 4 h at 450 °C) on a glass filtration rig under low vacuum pressure (< 10 mmHg). For DOC and TDN, samples were acidified (20 μL of 1:1 trace metal clean hydrochloric acid and Milli-Q water) in 20 mL glass vials with Teflon lined caps, prior to storage at 4 °C until laboratory analysis. These samples were stored acidified for preservation and to facilitate degassing of DIC during analysis; storing the samples in the same vials as were used during analysis also reduced the risk of contamination. For TDP, filtered samples were stored in 175 mL HDPE at −20 °C until laboratory analysis.

2.5. Dissolved organic carbon and total dissolved nitrogen analysis

Samples for measurement of dissolved organic carbon (DOC) and total dissolved nitrogen (TDN) were analysed onshore using high temperature catalytic oxidation (HTCO) on a Shimadzu TOC-V_{CPN}. The limits of detection for DOC and TDN were 3.4 μM and 1.8 μM, respectively, with a precision of 2.5%. Consensus Reference Materials were provided by D. Hansell (Miami, RMAS) were analysed daily with a mean and standard deviation for TDN and DOC of 32.9 ± 1.7 μM (expected range 32.25–33.75 μM) and 43.9 ± 1.2 μM (expected range 42–45 μM; n = 39), respectively. Concentrations of dissolved organic

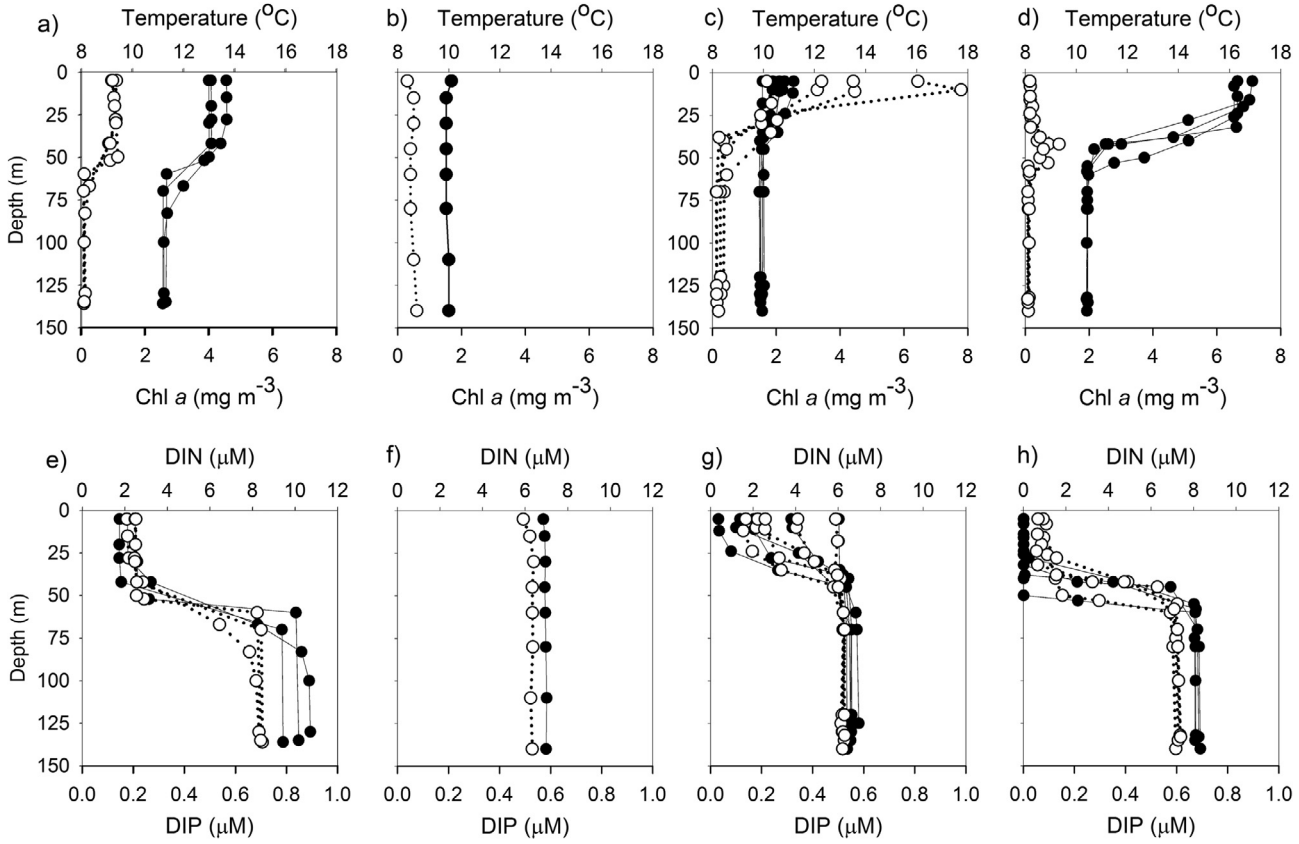

Fig. 2. Depth variation in temperature (°C; closed circles) and calibrated chlorophyll *a* fluorescence (Chl *a*, mg m^{-3}; open circles) at the Central Celtic Sea during (a) autumn (DY018), (b) winter (DY021), (c) spring (DY029) and (d) summer (DY033); and depth variation in dissolved inorganic nitrogen (DIN, μM; closed circles) and dissolved inorganic phosphorus (DIP, μM; open circles) at the Central Celtic Sea during (e) autumn (DY018), (f) winter (DY021), (g) spring (DY029) and (h) summer (DY033).

nitrogen (DON) were determined by subtracting the concentration of inorganic nitrogen (nitrate, nitrite, and ammonium) from TDN concentrations. Precision of analysis was better than 2% for DOC, and better than 3% for TDN, which together with the errors associated with inorganic nutrient concentrations resulted in precision of 5% for DON.

2.6. Total dissolved phosphorus analysis

Total dissolved phosphorus (TDP) was determined using the high temperature acid persulfate technique as described in Lomas et al. (2010) with the following modifications. Standards were made up in P-free artificial seawater using potassium monobasic phosphate ($KHPO_4$, Sigma Aldrich). Samples and standards were autoclaved (121 °C, 40 min) as 40-ml aliquots in tightly sealed 50-ml glass Pyrex® bottles with Teflon® lined screw caps after addition of 5-ml potassium persulfate solution (64 g/L). Following oxidation samples were left to cool overnight and then precipitated using the MAGIC technique (Karl and Tien, 1992) by addition of 5-ml 1 M NaOH solution (Sigma Aldrich). This step removed chloride ions, which appeared to cause interference during DIP determination. Following centrifugation (1000*g*, 60 min), the supernatant was discarded and the sample/standard pellet was completely dissolved in 40-ml 0.1 M HCl (Trace metal grade, Sigma Aldrich). Analytical blanks were determined as described in Lomas et al. (2010).

Total dissolved phosphorus was then determined in triplicate as dissolved inorganic phosphorus (DIP) concentrations in the samples by the molybdenum blue method (Murphy and Riley, 1962) using a Bran and Leubbe QuAAtro 5-channel autoanalyser (DIP detection limit 50 nM). Dissolved organic phosphorus (DOP) was quantified as the difference in DIP concentrations before and after persulfate oxidation (i.e. DOP = TDP − DIP; DOP detection limit 40 nM).

2.7. Statistics and calculations

All statistical tests were conducted using the SigmaPlot 13.0 software package. The Mann-Whitney rank sum test was used to determine whether groups of data were significantly different from one another, unless stated otherwise.

The depth of the base of the thermocline was calculated using high-resolution CTD data and was defined as the depth at which temperature deviated by > 0.05 °C from the deepest recorded temperature for a given profile. Below the base of the thermocline was defined as the bottom mixed layer (BML) and above the base of the thermocline was defined as the surface mixed layer (SML).

The rationale for using this definition was (a) timescale: the BML is isolated from atmospheric exchange while the SML is not, therefore the layers are different ages (b) light: the SML is within the euphotic layer and therefore can host primary production, while the BML experiences insufficient radiation to support primary production; (c) transport: the SML is subject to wind driven transport and inertial oscillations, while the BML is more strongly influenced by tidal currents. Using this definition, the seasonal subsurface chlorophyll maximum (SCM) associated with the thermocline was included in the SML.

Mean layer concentrations were obtained by depth integration of discrete concentration data across respective layers of the water column and normalisation to the layer thickness. These values are quoted with the standard deviation or 95% confidence interval (i.e. ‘mean ± S.D.’ or ‘mean ± 95% C.I.’), representing the variability between repeat casts during specific cruises.

3. Results

3.1. Seasonality in water column structure

In autumn 2014 (DY018) there was enhanced convective mixing in the SML due to surface cooling relative to the summer (Wihsgott et al., this issue). The base of the thermocline was deepest in autumn (mean ± S.D., 71 ± 10 m) with a weaker vertical nutrient gradient and higher DIN and DIP concentrations throughout the water column than were observed in summer 2015 (DY033, Fig. 2). Chl *a* concentrations were evenly dispersed throughout the SML in autumn ($\sim$1 mg m^{-3}), and were elevated relative to those observed during the summer cruise (Fig. 2) indicative of an autumn bloom. Mooring data presented in Wihsgott et al. (this issue) indicate that the CTD sampling campaign captured the development, peak and decline of the autumn bloom (Wihsgott et al., this issue). The highest BML temperatures (mean ± S.D., 11.2 ± 0.07 °C) and inorganic nutrient concentrations were observed during this cruise (mean ± S.D., 10.3 ± 0.7 μM DIN, 0.69 ± 0.02 μM DIP, $p < 0.001$) (Fig. 2).

In March 2015 (DY021), considered synonymous with winter conditions, the water column was well mixed with weak vertical structure in temperature (9.95 ± 0.08 °C) and near homogenous DIN (6.95 ± 0.05 μM), DIP (0.52 ± 0.01 μM), and Chl *a* concentrations (0.45 ± 0.09 mg m^{-3}) (Fig. 2). SML and BML layers were indistinguishable during this cruise as the water column was fully mixed.

During spring 2015 (DY029, Fig. 2) the water column began to stratify and an intense phytoplankton bloom developed in the SML, with Chl *a* concentrations reaching $\sim$8 mg m^{-3} (Fig. 2). Comparison with MODIS sea surface temperature and Chl *a* images suggest that these observations were due to the temporal progression of a bloom rather than lateral advection of water masses on station (C. Williams, Liverpool, pers. comm.). Surface layer DIN and DIP concentrations had decreased at the beginning of April (6.08 μM and 0.50 μM, respectively) relative to concentrations observed in March. During the spring bloom in April 2015, DIN and DIP concentrations in the SML rapidly decreased to 0.38 μM and 0.13 μM, respectively, within 21 days (Fig. 2). The depth of the base of the thermocline, synonymous with the depth of the SML, was 48 ± 9 m in the spring. BML temperature (9.92 ± 0.06 °C), DIN concentration (6.61 ± 0.17 μM) and DIP concentration (0.52 ± 0.004 μM) were similar to those of March 2015, but lower than those in autumn 2014 (Fig. 2).

In summer 2015, there was strong thermal stratification of the water column and DIN and DIP concentrations in the SML were low (below limit of detection and 0.06 μM, respectively; Fig. 2). The base of the thermocline was 54 ± 7 m with very strong vertical nutrient gradients and SCM within the lower thermocline (Fig. 2). Summertime BML temperature (10.43 ± 0.02 °C), DIN concentration (8.02 ± 0.37 μM) and DIP concentration (0.59 ± 0.03 μM μM) had increased relative to spring 2015 but were lower than those of autumn 2014 (Fig. 2).

3.2. Distribution and magnitude of particulate organic matter

To account for the variation in layer depth and the influence this had on the inventory presented in Table 1, mean layer concentrations were derived by normalisation to layer thickness (Fig. 3). POM concentrations were significantly higher in the SML than the BML when the water column was stratified ($p < 0.05$; autumn 2014, spring 2015, and summer 2015) but not when it was well mixed ($p > 0.2$; winter 2015) (Fig. 3). Layer-integrated values were also higher in the SML than the BML (Table 1), suggesting net production of POM in the SML and net consumption or loss of POM in the BML. Discrete POC and fluorescence-derived Chl *a* concentrations were strongly correlated ($p < 0.001$) during bloom events in autumn 2014 and spring 2015, suggesting a dominance of autotrophic biomass on POM distribution at these times. However, this relationship was slightly weaker in summer 2015 due to decoupling between POC and Chl *a* in the SCM ($p = 0.008$).

POM concentrations were highest in spring (Fig. 3), reaching maxima of 28 μM POC, 4 μM PON and 0.2 μM PPhos in the SML (data not shown); a 7-fold increase in POC and 6-fold increase in PON relative to winter concentrations (4.1 μM and 0.7 μM, respectively, data not shown). In the SML, POM concentrations were significantly lower in summer than spring ($p < 0.001$, Fig. 3). POC and PPhos concentrations were similar in autumn 2014 and summer 2015, while PON concentrations were significantly higher in autumn ($p < 0.001$, *t*-test, Fig. 3). In the BML, POM concentrations were highest in winter and spring 2015. The lowest POC and PPhos concentrations were observed in autumn 2014, while the lowest PON concentrations were observed in summer 2015 (Fig. 3). The difference in C, N and P distributions between cruises indicate decoupling of these pools over seasons.

3.3. Distribution and magnitude of dissolved organic matter

The DOM pool dominated the total organic pool (i.e. TOM = DOM + POM), with DOM accounting for 92–96% OC, 78–91% of ON, and 58–72% of OP (Table 1). C, N and P dynamics were decoupled in the DOM pool. In autumn, the vertical distribution of DOC and DON concentrations, which were significantly higher in the SML than the BML ($p < 0.001$, *t*-test, and $p = 0.04$, respectively), contrasted to the DOP distribution, where concentrations were highest in the BML ($p < 0.001$, *t*-test). In winter, DOC and DON had uniform vertical distributions as the water column was well mixed (68 μM and 4.0 μM, respectively). By spring, DOC and DOP concentrations were higher in the SML than the BML ($p = 0.003$ and $p = 0.006$, respectively, *t*-test), while DON concentrations did not vary significantly between layers ($p = 0.40$, *t*-test). In summer, this relation had reversed and DON concentrations were significantly higher in the SML than the BML ($p = 0.008$), while DOC and DOP concentrations did not vary significantly between layers ($p = 0.12$ and $p = 0.16$, respectively). However, the DOM inventory for the water column showed that BML values were higher than SML values throughout, often due to a greater layer thickness rather than higher concentrations (Table 1).

The seasonal signal in mean layer DOM concentrations were decoupled between the SML and BML and between the different nutrient pools. Mean layer concentrations of DOC were highest in the SML and BML in spring and lowest in summer and autumn, respectively, although differences were not significant (Fig. 3). DON concentrations were lowest in the SML in winter and highest in summer, and in the BML were highest in winter and lowest in spring (Fig. 3). DOP was highest in autumn and lowest in summer in both layers (Fig. 3). The different seasonal patterns in the organic C, N and P pools again suggests that the processes governing their distributions are decoupled from one another.

3.4. Short term and seasonal variability in organic matter dynamics

Shelf seas are highly dynamic regions on timescales of days (e.g. tides and wind driven mixing), to weeks (e.g. bloom events), to months (e.g. the seasonal cycle) and even years or more (e.g. variation in annual freshwater inputs and climate forcing). During sampling in autumn 2014 and spring 2015 there were bloom events associated with the breakdown- and initiation- of seasonal stratification, respectively (García-Martín et al., this issue; Wihsgott et al., this issue). Temporally resolved integrated water column values of POM and DOM within each of these cruises reflect the progressive change in OM pools associated with each bloom event, with evidence of decoupling between the different nutrient pools (Fig. 4).

In autumn, the organic C and N pools appeared coupled whilst their accumulation/loss was mirrored by opposing trends in the P pools (Fig. 4). Overall, during the period that the autumn bloom was sampled, there was an increase in POC and PON, but a decline in PPhos. DOC and DON values were highest on 21st November, when the DOP inventory was smallest (Fig. 4).

Table 1
Inventory of integrated organic nutrient values (mean ± 95% C.I., mmol m^{-2}).

Layer	Season	POC	DOC	PON	DON	DIN	PPhos	DOP	DIP
		mmol m^{-2}							
Total	Autumn	609 ± 56	9500 ± 583	135 ± 14	762 ± 134	1062 ± 75	3.1 ± 2.1	55 ± 6	76 ± 3
	Winter	617	10,062	111	749	1044	n.d.	n.d.	n.d.
	Spring	889 ± 117	9837 ± 658	162 ± 28	586 ± 127	804 ± 123	6.1 ± 1.9	42 ± 7	65 ± 8
	Summer	723 ± 115	9660 ± 246	77 ± 11	781 ± 9	839 ± 41	2.9 ± 0.7	26 ± 2	66 ± 3
SML	Autumn	377 ± 22	4592 ± 206	85 ± 9	360 ± 59	226 ± 99	1.8 ± 1.2	24 ± 0.2	18 ± 4
	Spring	504 ± 106	3158 ± 87	94 ± 25	190 ± 32	176 ± 63	3.4 ± 1.4	15 ± 1	16 ± 4
	Summer	388 ± 38	3545 ± 299	49 ± 8	323 ± 11	62 ± 38	1.7 ± 0.5	10 ± 2	9 ± 2
BML	Autumn	227 ± 23	4918 ± 386	53 ± 8	392 ± 88	805 ± 54	1.2 ± 1.0	34 ± 9	56 ± 1
	Spring	420 ± 64	7105 ± 205	74 ± 13	408 ± 80	695 ± 17	2.9 ± 0.8	29 ± 6	55 ± 0.2
	Summer	338 ± 87	6108 ± 49	29 ± 6	457 ± 18	775 ± 9	1.2 ± 0.3	16 ± 0.5	57 ± 1

†Note: Details provided include data for the total water column, surface mixed layer (SML) and bottom mixed layer (BML) in autumn (DY018), winter (DY021), spring (DY029) and summer (DY033) and at the Central Celtic Sea (CCS).

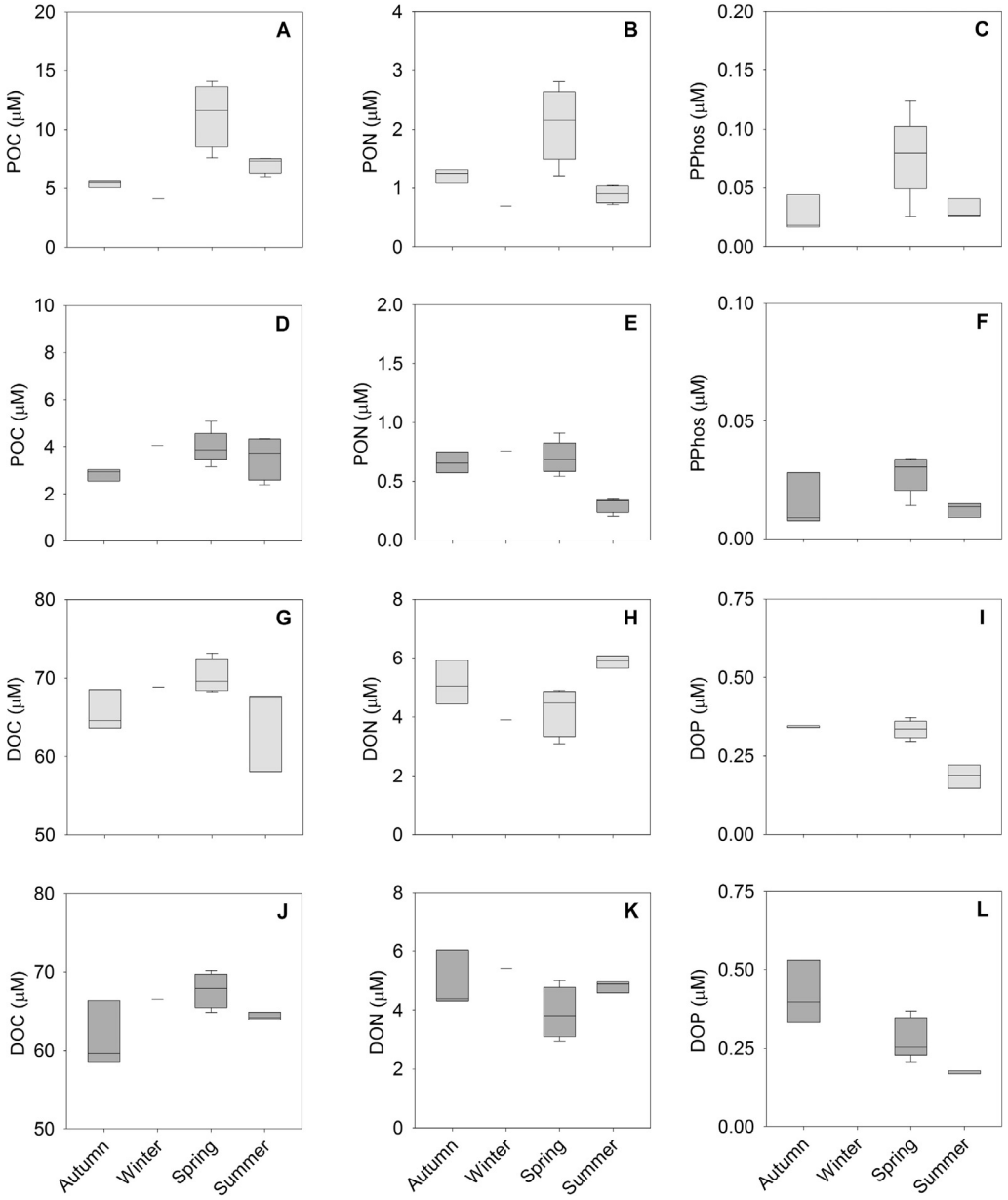

Fig. 3. Box plots of depth-averaged integrated concentrations (µM) of POC, PON, PPhos and DOC, DON and DOP in the surface mixed layer (light grey, A-C, G-I) and bottom mixed layer (dark grey, D-F and J-L) at the Central Celtic Sea in autumn (DY018), winter (DY021), spring (DY029), and summer (DY033). Boxes represent 95% C.I., whiskers represent 1 S.D. A summary of statistical *t*-test results is presented in Supplementary Table 1.

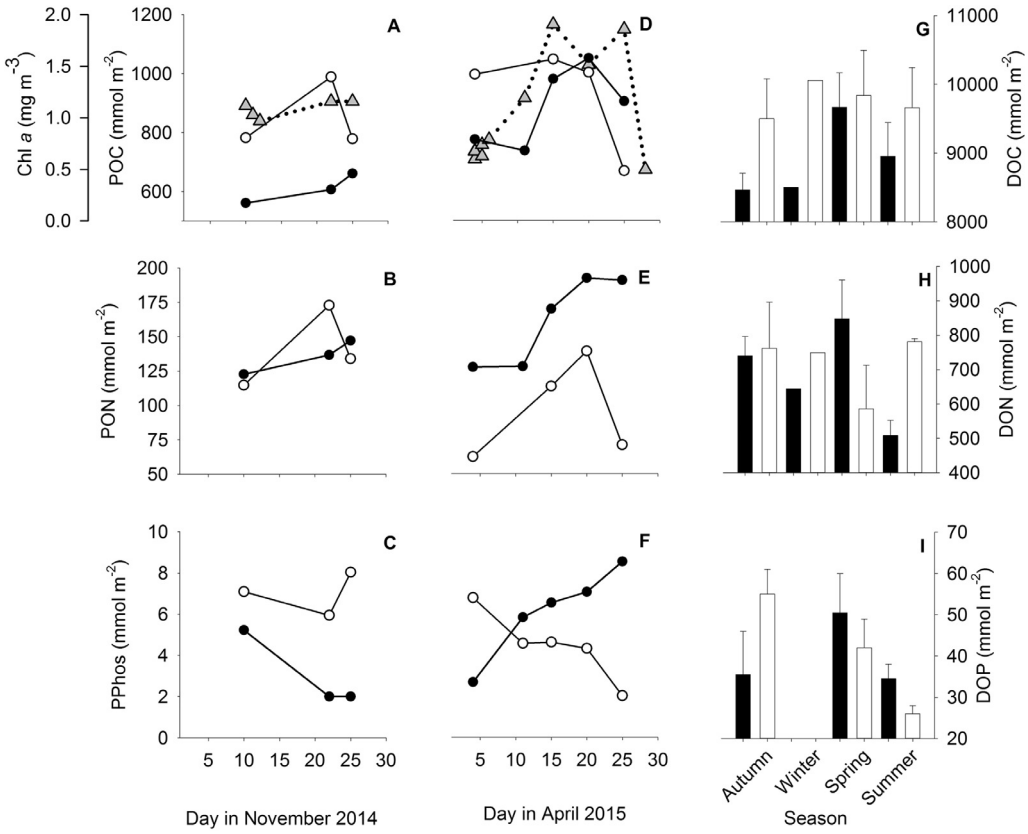

Fig. 4. Water column integrated values versus day of the month during November 2014 (autumn, DY018; A, B, C) and April 2015 (spring, DY029; D, E, F) for C, N and P particulate (closed circles) and dissolved (open circles) organic matter pools and mean SML Chl *a* concentration (grey triangles, mg m^{-3}) at the Central Celtic Sea site; and average integrated water column values for each cruise/season (mean ± 95% C.I.) for particulate (black bars) and dissolved (open bars) for organic C (G), N (H), and P (I) pools.

In spring, there was a 35% increase in POC over a 15-day period between the beginning of the cruise and the peak of the bloom, compared to a maximum seasonal range in POC of 46% increase between autumn and spring. PON increased by 51% and PPhos by 218% over the same period of the bloom (Fig. 4). Maximum accumulation rates in POC and PON were observed between 11th and 15th April (61 mmol C m^{-2} d^{-1} and 10 mmol N m^{-2} d^{-1}, respectively) and maximum rates of decline were observed between 20th and 25th April (−29.3 mmol C m^{-2} d^{-1} and −0.3 mmol M m^{-2} d^{-1}, respectively). By comparison, the highest PPhos accumulation rates were at the beginning and end of the sampling period (0.45 mmol P m^{-2} d^{-1} and 0.30 mmol P m^{-2} d^{-1}, respectively) and were lowest during the peak of the bloom (0.10 mmol P m^{-2} d^{-1}), while sustaining net accumulation throughout (Fig. 4).

Approaching the peak of the spring bloom there was a decoupling in the DOM pool with a decline in DOC, little change in DOP and an accumulation of DON. After the observed POC peak (20th April), there was a rapid decrease in DOM. DOC and DOP both decreased overall during the spring cruise, while DON was maximum on 20th April before declining rapidly to pre-bloom values.

Comparison of intra- and inter-cruise OM inventories suggests that a broad seasonal cycle may be evident for POC and PON, but that PPhos is far too dynamic on short timescales to exhibit a significant seasonal pattern (Fig. 4). There is no significant seasonal pattern in DOC, this is also broadly true of DON except for the contrast between low spring values and high summer values (Fig. 4). There was evidence of a seasonal cycle in the DOP pool, for example, inventory values were highest in autumn and significantly lower in summer (Fig. 4).

3.5. Variable organic matter stoichiometry in the Celtic Sea

Average POM stoichiometry for each cruise was coupled between the SML and the BML (Table 2). As such, both layers were most C rich relative to N and P in summer. Relative to C, POM was most P rich in spring and most N rich in autumn (Table 2).

DOM stoichiometry did not follow the same seasonal pattern as POM (Table 2). The SML and BML were coupled, exhibiting the same broad seasonal pattern. DOM was most C rich relative to P in summer and relative to N in spring, while relative to C it was most P rich in autumn (Table 2). The C:N stoichiometry of the DOM pool was very similar in summer and autumn, with the pool being most N rich relative to C in summer for the SML and autumn for the BML (Table 2). The DOM pool was more C rich in the BML than the SML in summer, but this was only significant for C:N (Table 2), otherwise there was no significant vertical variation in DOM stoichiometry.

Relative to P, TOM stoichiometry was most C rich in summer and C poor in autumn. While relative to N, it was most C rich in spring and most C poor in autumn (Table 2). The C:P TOM stoichiometry was significantly higher in the BML than the SML in summer ($p < 0.05$), otherwise there was no significant vertical variation in stoichiometry (Table 2).

Considerable short-term variability in OM stoichiometry was observed during bloom events in autumn 2014 and spring 2015 (Fig. 5). This variability was comparable to the inter-cruise variability that was considered synonymous with the seasonal cycle. Within each bloom cruise, POM stoichiometry was more variable than DOM stoichiometry, with the exception of C:N stoichiometry (Fig. 5). The C:P stoichiometry of the particulate and dissolved pools were most similar, while N:P stoichiometry indicated that particles were always N-rich relative to the dissolved phase, and C:N suggested that the dissolved phase was C-rich relative to particles (Fig. 5).

Focussing on inter-cruise comparisons, the coupling between stoichiometry of the particulate and dissolved pools was strongest for C:P, with coincident maximum and minimum C:P stoichiometry occurring during the same cruises for both POM and DOM pools (Fig. 5). There were few significant differences in stoichiometric values involving P due to large variability of the organic P pools within cruises. However, C:N stoichiometry showed that the DOM pool was significantly more C

Table 2
Summary of integrated organic nutrient stoichiometry (mean ± 95% C.I.) and integrated organic plus inorganic stoichiometry (Total N:P).

Layer	Season	POM			DOM			TOM			TOTAL
		C:P	N:P	C:N	C:P	N:P	C:N	C:P	N:P	C:N	N:P
Total	Autumn	198 ± 137	44 ± 31	4.5 ± 0.1	172 ± 29	14.0 ± 3.8	12.5 ± 1.5	174 ± 31	15.4 ± 4.2	11.3 ± 1.2	14.3 ± 0.9
	Winter			5.6			13.4			12.4	
	Spring	145 ± 63	26 ± 9	5.6 ± 0.4	234 ± 36	14.4 ± 3.7	17.0 ± 3.4	222 ± 84	15.4 ± 6.0	14.3 ± 4.2	13.8 ± 1.4
	Summer	247 ± 40	26 ± 4	9.4 ± 2.1	366 ± 22	29.7 ± 2.2	12.4 ± 0.2	354 ± 14	29.2 ± 1.6	12.1 ± 1.8	17.8 ± 0.5
SML	Autumn	205 ± 136	47 ± 33	4.4 ± 0.2	191 ± 10	15.0 ± 2.5	12.8 ± 1.7	192 ± 15	17.2 ± 3.3	11.2 ± 1.4	15.2 ± 0.9
	Spring	146 ± 65	27 ± 9	5.4 ± 0.5	209 ± 11	12.6 ± 2.3	16.6 ± 4.0	198 ± 73	15.3 ± 5.1	12.9 ± 4.2	13.8 ± 1.2
	Summer	226 ± 54	29 ± 4	7.8 ± 0.8	347 ± 44	31.7 ± 7.9	11.0 ± 1.2	330 ± 29	31.2 ± 5.9	10.6 ± 2.0	21.2 ± 10
BML	Autumn	191 ± 178	44 ± 42	4.3 ± 0.3	147 ± 50	11.7 ± 5.9	12.5 ± 1.7	148 ± 51	12.8 ± 6.2	11.6 ± 1.3	13.9 ± 6.6
	Spring	144 ± 64	25 ± 11	5.7 ± 0.4	241 ± 60	13.9 ± 4.5	17.4 ± 3.3	232 ± 102	14.9 ± 6.7	15.6 ± 4.4	13.8 ± 1.5
	Summer	283 ± 25	24 ± 11	11.6 ± 5.9	377 ± 14	28.2 ± 1.1	13.4 ± 0.6	371 ± 12	27.9 ± 1.7	13.3 ± 1.9	16.9 ± 3.4

†Note: Details provided include data for the whole water column (total), surface mixed layer (SML) and bottom mixed layer (BML) in autumn (DY018), winter (DY021), spring (DY029) and summer (DY033). A summary of statistical *t*-test results is presented in Supplementary Table 2.

rich throughout the year relative to POM C:N stoichiometry, excluding summer when both pools become N rich (Fig. 5).

3.6. Suspended and sinking particulate organic matter

The MSC separated the POM pool based on sinking speed into POM_{susp}, POM_{slow} (allowing derivation of $POM_{slow\text{-}susp}$) and POM_{fast}. POM_{susp} and POM_{fast} concentrations were highest in the SML and BML in spring, while $POM_{slow\text{-}susp}$ concentrations were highest in both layers in autumn (Table 3).

POM_{fast} was C poor relative to POM_{susp} throughout sampling; as was POM_{slow} compared to POM_{susp} except for the autumn BML and the summer SML values (Table 3). POM_{susp} was most C rich relative to N in summer in the SML and in spring in the BML, and was most C poor in autumn. The highest SML and BML POM_{slow} C:N stoichiometric values were in summer and autumn, respectively. For POM_{fast} there was negligible seasonal variation in C:N stoichiometry, which remained low (< 6) (Table 3).

4. Discussion

There are set conditions for organic matter dynamics that would suggest that seasonal bloom events favour net production of fresh OM of relatively labile nature, reflected by stoichiometric values closer to Redfield than that of refractory material (Carlson and Hansell, 2014). Conversely, periods of strong stratification and associated inorganic

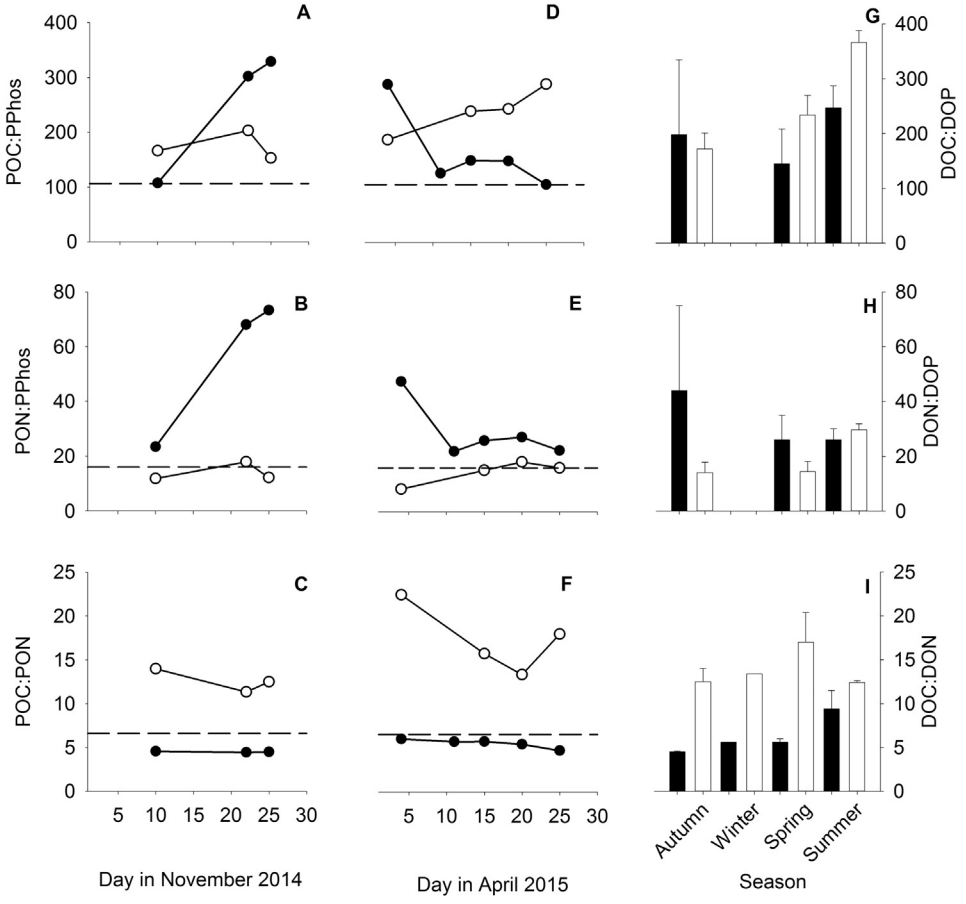

Fig. 5. Stoichiometry of integrated water column inventories versus day of the month for November 2014 (autumn, DY018; A, B, C) and April 2015 (spring, DY029; D, E, F) for C:P, N:P and C:N particulate (closed circles) and dissolved (open circles) organic matter pools; and summary of particulate (black bars) and dissolved (open bars) integrated organic nutrient stoichiometry for each cruise/season (mean ± 95% C.I.) for C:P (G), N:P (H), and C:N (I). The dashed line indicates Redfield stoichiometry (Redfield et al., 1963).

Table 3
Summary of mean particulate organic carbon (POC, μM, mean ± 95% C.I.) and the associated carbon to nitrogen (C:N, mean ± 95% C.I.) stoichiometry at the Central Celtic Sea station.

Layer	Season	POC_{susp}	POC_{slow}	$POC_{slow\text{-}susp}$	POC_{fast}	$C:N_{susp}$	$C:N_{slow}$	$C:N_{fast}$
		(μM)						
SML	Autumn	6.8 ± 0.9	10.0 ± 7.3	3.2 ± 6.4	0.22 ± 0.13	5.6 ± 0.7	6.3 ± 1.2	5.1 ± 0.8
	Spring	20.7 ± 5.5	19.2 ± 7.4	1.6 ± 4.8	0.67 ± 0.65	5.8 ± 0.1	5.4 ± 1.4	5.4 ± 4.3
	Summer	9.2 ± 2.3	7.6 ± 1.8	1.6 ± 1.5	0.27 ± 0.10	6.3 ± 1.4	8.4 ± 3.5	4.2 ± 0.9
BML	Autumn	2.5 ± 1.1	7.5 ± 9.9	4.2 ± 10.8	0.12 ± 0.20	5.4 ± 1.6	7.5 ± 3.3	4.4 ± 4.0
	Spring	7.0 ± 3.8	5.2 ± 0.3	1.8 ± 3.9	0.52	7.6 ± 4.8	5.3 ± 0.8	4.6
	Summer	5.8 ± 3.0	4.6 ± 1.5	1.2 ± 1.9	0.22 ± 0.01	6.1 ± 2.1	5.6 ± 1.7	4.6 ± 1.2

†Note: Details provided include POC concentrations and C:N stoichiometry in the surface mixed layer (SML) and bottom mixed layer (BML) for the suspended (POM_{susp}), slow sinking (POM_{slow}), suspended-corrected slow sinking ($POM_{slow\text{-}susp}$), and fast sinking (POM_{fast} particle fractions. Seasons correspond to DY018 (autumn), DY029 (spring), and DY033 (summer); the marine snow catcher was not deployed during DY021 (winter). A summary of statistical *t*-test results is presented in Supplementary Table 3.

nutrient limited production favour depletion of an OM pool, which may become progressively C rich through utilisation as a nutrient and energy source by microbes (Jiao et al., 2010) and through photodegradation over time in the SML (Moran and Zepp, 1997). In addition, OM production may become more C rich due to C overconsumption (Kähler and Koeve, 2001) and OM production stoichiometry reflective of ambient nutrient availability, for example, in a DIP-stressed population DOM production is P-poor (Conan et al., 2007).

A striking feature of the Celtic Sea is how both short term and seasonal temporal changes in DOP had opposing trends to PPhos (Figs. 3 and 4). When the particulate pool increased, the dissolved pool decreased and *vice versa*. In contrast, the dissolved and particulate OC pools were coupled and increased or decreased at the same time (Fig. 4); this was also true of ON except for summer. Furthermore, the particulate C and N pools appear to be closely coupled, while PPhos behaves quite differently during bloom conditions in this region, as has previously been reported (Davis et al., 2014). Together, these observations provide circumstantial evidence for a heavy dependence of OM dynamics on nutrient status in this DIN-limited environment (Poulton et al., this issue). The DOM pool was generally more C rich than the POM pool. For C:N this was most pronounced during bloom periods, while for C:P this was most pronounced in the nutrient-stressed summer (Fig. 5).

4.1. Seasonal variation in organic matter in the Celtic Sea

To examine OM dynamics in the Celtic Sea, we undertook a series of sampling campaigns during autumn (2014), winter, spring and summer (2015) to represent different stages of the seasonal cycle. The magnitude of the POM pool showed strong seasonal variation linked to nutrient and light availability, with POM maxima during the spring bloom when inorganic nutrients were replete and light limitation, which was characteristic of winter conditions, was alleviated (Figs. 2 and 3). PON and PPhos minima were observed in summer when primary production was limited by DIN availability, and a POC minimum was observed in winter when production was limited by light (Table 1) (Poulton et al., this issue). Elevated POM concentrations in the SML versus the BML and a positive correlation between POC and Chl *a* suggest a strong autotrophic influence on POM distribution.

Here we consider the change in OC during a bloom event to represent freshly produced OC, thereby omitting the residual refractory pool from the following estimates. During a 4-day period at the peak of the spring bloom, net primary production (NPP) increased from 154 mmol C m^{-2} d^{-1} to 532 mmol C m^{-2} d^{-1} (Poulton et al., this issue). Assuming a linear transition and that NPP resulted in an increase in POC biomass, this implies an average NPP over the 4-day period of 343 mmol C m^{-2} d^{-1}, representing how much OC was being produced in the SML. Over the same period, POC accumulation rates reached 61 mmol C m^{-2} d^{-1} coinciding with a DOC accumulation rate of 20 mmol m^{-2} d^{-1} (Fig. 4). DOC production was likely derived from autotrophic biomass via exudation, lysis and grazing processes (Carlson, 2002). Together, accumulation of POC and DOC account for ~81 mmol C m^{-2} d^{-1} of the estimated NPP production. An additional term, in this case a loss term from the SML, was associated with the fast sinking POC flux. This was estimated to be 8.0 ± 7.8 mmol C m^{-2} d^{-1} (following Riley et al., 2012). Therefore, ~89 mmol C m^{-2} d^{-1} of OC produced by NPP can be accounted for by our observations, leaving an unaccounted deficit of ~254 mmol m^{-2} d^{-1}.

Community respiration is the conversion OM to CO_2. Where primary production rates (i.e. OC production) exceed community respiration rates (i.e. OC consumption), there is potential for net export of C (Wilson et al., 2014). García-Martín et al. (this issue) report community respiration rates of < 165 ± 5 mmol O_2 m^{-2} d^{-1} during the spring bloom (García-Martín et al., this issue). Here, we apply a yield respiration coefficient of 1.45 for average marine plankton ($C_{106}H_{177}O_{37}N_{17}S_{0.4}P_1$, Hedges et al., 2002), accepting the caveats of this simplified assumption when applied to this system (Middelburg et al., 2004), to estimate a community C consumption rate of 245 ± 7 mmol C m^{-2} d^{-1}. This value is similar to the POC loss term of ~254 mmol m^{-2} d^{-1} suggesting that the estimated deficit in the POC pool was potentially sufficient to meet community respiration demands. Thus, we speculate that fresh, labile, autochthonous POC, either directly or indirectly via a DOC intermediate, was an important substrate from microbial respiration and remineralisation processes in the SML during this period of net autotrophy. This allowed net production and accumulation of DOC, resulting in the observed seasonal maximum. However, by summer (< 3 months) this DOC maximum associated with the spring bloom had decayed, similar to observations from the North Sea (Johnson et al., 2013) and other ocean systems (Carlson et al., 1994).

DOM dominated the total organic matter pool (TOM), with DOC representing 92–94% of OC, DON representing 78–91% of ON, and DOP representing 58–72% of OP (Table 1). For the DOM pool, the range in seasonal mean concentrations expressed as a percentage of the lowest seasonal mean value (derived from Fig. 3) varied from ~7% for DOC, ~50% for DON to ~80% for DOP. Mean DOC concentrations ranged from ~65 to 70 μM, with a winter value of 69 μM (Fig. 3). In winter, up to 35% of DOC was from riverine sources (Carr et al., this issue), which equates to ~24 μM, plus ~44 μM of refractory DOC advected on-shelf from the Northeast Atlantic (Kähler and Koeve, 2001; Ogawa and Tanoue, 2003) during winter mixing, giving a total estimate of ~66 μM of allochthonous DOC, a large portion of which may have been refractory. This suggests that the observed minimum in DOC concentrations in the SML in summer may be largely refractory with rapid turnover of any labile fraction coinciding with net consumption of DOC by bacteria (García-Martín et al., this issue), and the ~7% increase in DOC concentrations observed in spring may represent the labile or semi-labile DOC pool as DOC production rates were highest in spring (García-Martín et al., this issue).

By comparison, the DOP mean concentrations in the SML ranged

from 0.19 to 0.35 μM (Fig. 3). This large relative seasonal range in mean SML concentration of ~80% suggests that this pool is proportionally much more labile than the DOC pool (Carlson and Hansell, 2014). DOP concentrations broadly reflected DOP production rates, which were highest in spring, then autumn and lowest in summer (Poulton et al., this issue). During the spring bloom the range in magnitude of P inventories was of similar order to the seasonal range. Opposing trends in DOP and PPhos during stages of the bloom suggested that DOP was of a labile nature and a potentially important source of P for heterotrophic and secondary production processes (Popendorf and Duhamel, 2015). Low summer DOP production rates (0.05 mmol P m^{-2} d^{-1}; Poulton et al., this issue) were of a similar magnitude to alkaline phosphatase rates previously reported for this region in summer (0.01–0.03 mmol m^{-2} d^{-1}; Davis et al., 2014). This suggests minimal potential accumulation rates of labile DOP esters in summer, potentially explaining the seasonal minimum in DOP in summer.

DON concentrations were at their highest in the SML in summer (~6 μM; Fig. 3) and at their lowest in winter (~3.9 μM; Fig. 3). These values are low but within the average range reported for coastal and continental shelf systems (9.9 ± 8.1 μM, Bronk, 2002), and similar to those reported for the Celtic Sea in January 2013 (1.0–3.7 μM, Moschonas et al., 2015) and the adjacent English Channel (4.5–10.1 μM, Butler et al., 1979). Elevated DON concentrations in summer have been previously reported for temperate shelf seas (Butler et al., 1979; Van Engeland et al., 2010; Johnson et al., 2013; Moschonas et al., 2015) and may be attributed to the productive season (Moschonas et al., 2015), lateral transfer from coastal regions (Van Engeland et al., 2010), seasonal changes in community structure (Butler et al., 1979), changes in water column structure and mixing (Moschonas et al., 2015) and changes in the partitioning of dissolved N as DIN is drawn down in the SML (Butler et al., 1979). The TDN inventory for the water column decreased during our sampling campaign from autumn 2014 (1824 ± 108 mmol m^{-2}, Table 1) to summer 2015 (916 ± 30 mmol m^{-2}, Table 1) suggesting that the system was not closed and that N was being lost, for example through reduced inputs, denitrification, sedimentation, or changes in water masses (Johnson et al., 2013). Humphreys et al. (this issue) found that the dissolved C inventory was also not in a steady state over the seasonal cycle sampled by this programme, a situation that has previously been reported for the North Sea (Chaichana et al., 2017).

4.2. How does variable OM stoichiometry influence the CSP?

The relative efficiency of the role of OM in the CSP is reliant on a decoupling of OM production stoichiometry and regeneration stoichiometry, allowing recycling of N and P to support further regenerated production in the SML and the accumulation of C in the OM pool. Within the OM component of the CSP, this C rich OM must ultimately either be transferred off shelf or remineralised to DIC below the seasonal thermocline in isolation from atmospheric exchange (Simpson and Sharples, 2012).

In the Celtic Sea, the DOM pool was much more C rich than the POM pool (Table 2). There are many factors that influence both POM and DOM stoichiometry, including nutrient status and growth stage (Arrigo, 2005; Conan et al., 2007), C overconsumption (Toggweiler, 1993), changes in community composition (Biddanda and Benner, 1997; Duhamel and Moutin, 2009), degradation processes (Hedges et al., 2001) and mechanisms of DOM production, e.g. viral cell lysis (Jiao et al., 2010). Perhaps the strongest influence in deviations from Redfield is the processing of DOM within the microbial loop (Azam et al., 1983; Jiao et al., 2010), as DOM typically has a longer residence time in the water column than POM (Hedges, 1992; Chin et al., 1998).

There was little seasonal variability in the C:N stoichiometry of the OM pool (Table 2). The mean C:N ratios of DOM (~12–17, Table 2) were comparable to those previously reported for the Celtic Sea (Davidson et al., 2013), North Sea (Van Engeland et al., 2010; Chaichana et al., 2017) and other shelf seas (Hopkinson et al., 1997). The Celtic Sea is N-limited in summer (e.g. Pemberton et al., 2004), thus the C and N pools were closely coupled as any increase in N could fuel more production. A dominance of *Synechococcus* during summer in the Celtic Sea has previously been reported (Moore et al., 2006), which have high C:N biomass due to C retention and release of C poor DOM (Biddanda and Benner, 1997). If this is a consistent feature of the Celtic Sea in summer, this may explain the elevated C:N of POM and suppressed C:N of DOM observed in this study (Table 2).

The C and P pools were not closely coupled and it was changes in P pools that were driving changes in OM stoichiometry. The lowest inorganic nutrient concentrations were observed in summer when DIP concentrations were still > 0.06 μM, while DIN concentrations were < 0.02 μM. This suggests that DIP availability did not limit primary production (Mahaffey et al., 2014) and therefore greater variability was observed in C:P and N:P stoichiometry than C:N stoichiometry.

In the current study the OM pool was most C rich relative to P in summer (Table 2). There are many factors that influence C:P stoichiometry. For example, during bloom events, decreases in C:P and N:P may indicate increased microbial demand for P for growth machinery, e.g. RNA (Arrigo, 2005; Klausmeier et al., 2008) and increased bacterial abundance (Duhamel and Moutin, 2009). When production is nutrient limited during strong seasonal stratification biomass stoichiometry may become P poor due to an increased N requirement for resource acquisition machinery, e.g. proteins and chlorophyll (Arrigo, 2005). Throughout a seasonal cycle, heterotrophic processes can drive preferential remineralisation of P relative to C and N causing C:P and N:P values to deviate from Redfield (Clark et al., 1998; Kolowith et al., 2001).

However, during this sampling campaign we observed a linear decrease in the total P inventory between autumn 2014 and summer 2015 from ~134 mmol P m^{-2} to ~95 mmol P m^{-2} ($p < 0.05$, data not shown). Across the same period the OC inventory increased by only ~3% and the ON inventory decreased by ~5%, suggesting that changes in the P pool were driving the stoichiometric signal of high C:P and high N:P OM in summer. Cross shelf gradients in salinity, DIN and DIP (Carr et al., this issue; Humphreys et al., this issue) suggest a near linear inverse relationship between DIP and salinity, while the central shelf region appears to act as a sink of DIN (Humpreys et al., this issue; Carr et al., this issue). This suggests that P dynamics were more strongly influenced by changes in water masses, while N dynamics were more strongly influenced by *in situ* processes such as internal cycling, regeneration and denitrification (Johnson et al., 2012), in addition to continual remineralisation of both nutrients (Humphreys et al., this issue).

4.3. How does the role of sinking POM compare to that of DOM in the CSP?

Zooplankton have an important role in the efficiency of the biological C pump through particle grazing, fragmentation and diel vertical migration (Cavan et al., 2017). Zooplankton faecal pellets are a common source of fast sinking POM (Cavan et al., 2015), with grazing typically preserving the elemental stoichiometry of prey (Plum et al., 2015). However, sinking POM C:N was always < 6 despite bulk POM C:N stoichiometry exceeding 6 in summer (Tables 2 and 3). In autumn, the zooplankton community was diverse and included nauplii, copepodites, and non-crustacean macrozooplankton with a dominance of predatory species in the mesozooplankton species (Giering et al., this issue). Slow sinking POM concentrations were at their highest during this cruise, and had elevated C:N stoichiometry relative to POM_{susp} and POM_{fast} (Table 3). Together these observations suggest that the grazing community did have some influence on the characteristics and elemental stoichiometry of sinking POM. Estimates of POC_{fast} fluxes were 2.6 ± 1.5 mmol C m^{-2} d^{-1} in autumn, 8.0 ± 7.8 mmol C m^{-2} d^{-1} in

spring, and 3.2 ± 1.2 mmol C $m^{-2} d^{-1}$ in summer (following Riley et al., 2012) with a C:N stoichiometry of 5.1 ± 0.8, 5.4 ± 4.3 and 4.2 ± 0.9, respectively (Table 3).

DOM stoichiometry deviated significantly from Redfield throughout our sampling campaign with DOC concentrations greatly exceeding POC concentrations. A vertical gradient in DOC concentration between the SML and the BML would facilitate a diapycnal flux of DOC to be transferred down the concentration gradient. A rough estimate of this vertical flux can be obtained using turbulent kinetic dissipation (K_z), or vertical turbulent mixing, values and the vertical gradient in DOC concentration (Williams et al., 2013). Average K_z values were obtained during the spring and summer cruise using autonomous gliders ($5 \times 10^{-5} m^{-2} s^{-1}$ and $8 \times 10^{-5} m^{-2} s^{-1}$, respectively; C Williams, Liverpool, pers. comm.), but not autumn. The DOC gradient was calculated from the average vertical DOC profile per cruise (Supplementary Fig. 1) as the gradient between the shallowest data point in the BML and the deepest data point in the SML; this was calculated to be 0.7 μM C m^{-1} in spring and 1.3 μM C m^{-1} in summer. These values together with the average K_z derived from the glider data, gave downward DOC flux estimates of 3.0 mmol C $m^{-2} d^{-1}$ in spring and 9.0 mmol C $m^{-2} d^{-1}$ in summer with C:N stoichiometry of 17 ± 3 and 12 ± 0.2, respectively (Table 2).

Thus, we conclude that the sinking POC flux is the dominant mechanism transferring OC below the thermocline during the spring bloom and that the diapycnal DOC flux is the dominant transfer mechanism during the summer period of enhanced stratification and nutrient limited production in the SML. However, in terms of CSP efficiency the stoichiometry of the DOM pool always exhibited the largest C rich deviation from Redfield suggesting that this pool may play an important role in sustaining efficient removal of C from the SML, while retaining N and P to support further regenerated production. The C rich DOM pool may provide an efficient export vehicle of C from the shelf to the open ocean during off-shelf transport of water during winter advection.

5. Conclusions

Shelf seas are highly productive regions with large C inventories. For OM to directly play a significant role in the shelf sea C export, a residual C rich OM pool is required. The spring bloom was a definitive point in the seasonal cycle, acting as a temporal hot spot for POM production and establishing a significant pool of OM that could then act as a food source for zooplankton, a nutrient and C source for bacteria or a potential vehicle for export of OM from the shelf sea.

DOM was the dominant OC pool and was always C-rich relative to the Redfield ratio (106C:16N:P, Redfield et al., 1963) and the POM pool. For C:N this was most pronounced during bloom periods, while for C:P this was most pronounced in the nutrient-stressed summer. This highlights a striking feature of the Celtic Sea: how the nutrient pools behave differently from one another. The particulate and dissolved OP pools followed opposing trends (i.e. an increase in POM was met with a decrease in DOM and *vice versa*), while for OC they were coupled and increased or decreased in step; this was also true for ON except in summer. Furthermore, the particulate C and N pools were closely coupled, while PPhos behaved quite differently during bloom conditions.

OC fluxes from the SML to the BML showed some seasonal dependence with the POC flux dominating during the spring bloom, and the DOC flux dominating during the stratified summer. Together, these observations provide circumstantial evidence for a heavy dependence of OM dynamics on nutrient status and water column structure in this shelf sea system.

Acknowledgements

This work was supported by the UK Natural Environment Research Council (NERC) grant NE/K0020007/1. We thank principal scientists, colleagues, captain and crew on RRS Discovery (cruises DY018, DY021, DY029 and DY033) and Dr. L. Darroch at the British Oceanographic Data Centre (BODC). We are indebted to two anonymous reviewers whose constructive feedback helped us to improve this paper.

Appendix A. Supplementary material

Supplementary data associated with this article can be found, in the online version, at http://dx.doi.org/10.1016/j.pocean.2018.02.021.

References

Amon, R.M.W., Benner, R., 1996. Bacterial utilization of different size classes of dissolved organic matter. Limnol. Oceanogr. 41 (1), 41–51.
Arrigo, K.R., 2005. Marine microorganisms and global nutrient cycles. Nature 437, 349–355. http://dx.doi.org/10.1038/nature04159.
Azam, F., Fenchel, T., Field, J.G., Gray, J.S., Meyer-Reil, L.A., Thingstad, F., 1983. The ecological role of water-column microbes in the sea*. Mar. Ecol. Prog. Ser. 10, 257–263.
Barron, C., Duarte, C.M., 2015. Dissolved organic carbon pools and export from the coastal ocean. Global Biogeochem. Cyc. 29 (10), 1725–1738. http://dx.doi.org/10.1002/2014GB005056.
Bauer, J., Cai, W.J., Raymond, P.A., Bianchi, T., Hopkinson, C.S., Regnier, P., 2013. The changing carbon cycle of the coastal ocean. Nature Rev. 504, 61–70.
Benner, R., 2003. Molecular indicators of bioavailability of dissolved organic matter. In: Findlay, S., Sinsabaugh, R.L. (Eds.), Aquatic Ecosystems: Interactivity of Dissolved Organic Matter. Academic Press, San Diego, pp. 121–135.
Biddanda, B., Benner, R., 1997. Carbon, nitrogen, and carbohydrate fluxes during the production of particulate and dissolved organic matter by marine phytoplankton. Limnol. Oceanogr. 42 (3), 506–518. http://dx.doi.org/10.4319/lo.1997.42.3.0506.
Bronk, D.A., 2002. Dynamics of DON. In: Hansell, D.A., Carlson, C.A. (Eds.), Biogeochemistry of Marine Dis- solved Organic Matter, first ed. Academic Press, San Diego, CA, pp. 153–247. http://dx.doi.org/10.1016/B978- 012323841-2/50007-5.
Butler, E., Knox, S., Liddicoat, M., 1979. The relationship between inorganic and organic nutrients in sea water. J. Mar. Bio. Ass. UK 59, 239–250.
Carlson, C.A., 2002. Production and removal processes. In: Hansell, D.A., Carlson, C.A. (Eds.), Biogeochemistry of Marine Dissolved Organic Matter. Academic Press, Santa Barbara, Calif, pp. 91–151.
Carlson, C.A., Hansell, D.A., 2014. DOM sources, sinks, reactivity and budgets, second ed. Elsevier Inc, pp. 65–126. http://dx.doi.org/10.1016/B978-0-12-405940-5.00003-0.
Carlson, C.A., Ducklow, H.W., Hansell, D.A., Smith, W.O., 1998. Organic carbon partitioning during spring phytoplanktonblooms in the Ross Sea polynya and the Sargasso Sea. Limnol. Oceanogr. 43 (3), 375–386. http://dx.doi.org/10.4319/lo.1998.43.3.0375.
Carlson, C.A., Ducklow, H.W., Michaels, A.F., 1994. Annual flux of dissolved organic carbon from the euphotic zone in the northwestern Sargasso Sea. Nature 371, 405–408. http://dx.doi.org/10.1038/371405a0.
Carr, N., Davis, C.E., Blackbird, S., Daniels, L.R., Preece, C., Woodward, E.M.S., Mahaffey, C., this issue. Seasonal and spatial variability in the source and characteristics of DOM in a temperate shelf sea. Prog. Oceanogr.
Cavan, E.L., Le Moigne, F.A.C., Poulton, A.J., Tarling, G.A., Ward, P., Daniels, C.J., Fragoso, G.M., Sanders, R.J., 2015. Attenuation of particulate organic carbon flux in the Scotia Sea, Southern Ocean, is controlled by zooplankton fecal pellets. Geophys. Res. Let. http://dx.doi.org/10.1002/2014GL062744.
Cavan, E., Trimmer, M., Shelley, F., Sanders, R., 2017. Remineralization of particulate organic carbon in an ocean oxygen minimum zone. NatureComms. 8, 14847. http://dx.doi.org/10.1038/ncomms14847.
Cembella, A.D., Antia, N.J., Harrison, P.J., 1984. The utilization of inorganic and organic phosphorus compounds as nutrients by eukaryotic microalgae: a multidisciplinary perspective: part 2. Crit. Rev. Microbiol. 11 (1), 13–81.
Chaichana, S., Jickells, T., Johnson, M., 2017. Distribution and C/N stoichiometry of dissolved organic matter in the North Sea in summer 2011–12. Biogeosceinces Discuss. http://dx.doi.org/10.5194/bg-2017-387.
Chin, W.C., Orellana, M.V., Verdugo, P., 1998. Spontaneous assembly of marine dissolved organic matter into polymer gels. Nature 391, 568–572. http://dx.doi.org/10.1038/3545.
Clark, L.L., Ingall, E.D., Benner, R., 1998. Marine phosphorus is selectively remineralised. Sci. Correspond. Nat. 393, 426.
Conan, P., Sondergaard, M., Kragh, T., Thingstad, F., Puji-Pay, M., Williams, P.J.B., Markager, S., Cauwet, G., Borch, N.H., Evans, D., Riemann, B., 2007. Partitioning of organic production in marine plankton communities: the effects of inorganic nutrient ratios and community composition on new dissolved organic matter. Limnol. Oceanogr. 52 (2), 753–765.
Davidson, K., Gilpin, L.C., Pete, R., Brennan, D., McNeill, S., Moschonas, G., Sharples, J., 2013. Phytoplankton and bacterial distribution and productivity on and around Jones Bank in the Celtic Sea. Prog. Oceanogr. 117, 48–63.
Davis, C.E., Mahaffey, C., 2017. Elevated alkaline phosphatase activity in a phosphate-replete environment: influence of sinking particles. Limnol. Oceanogr. http://dx.doi.org/10.1002/lno.10572.
Davis, C.E., Mahaffey, C., Wolff, G.A., Sharples, J., 2014. A storm in a shelf sea: variation in phosphorus distribution and organic matter stoichiometry. Geophys. Res. Lett.

http://dx.doi.org/10.1002/2014GL061949.
De Leeuw, J.W., Largeau, C., 1993. A review ofmacromolecular organic compounds that comprise living organisms and their rolein kerogen, coal, and petroleum formation. In: Organic Geochemistry. Springer, Boston, MA, pp. 23–72.
Ducklow, H.W., 2000. Bacterial production and biomass in the oceans. In: Kirchman, D.L. (Ed.), Microbial Ecology of the Oceans. Wiley- Liss, New York, pp. 85–120.
Duhamel, S., Moutin, T., 2009. Carbon and phosphate incorporation rates of microbial assemblages in contrasting environments in the Southeast Pacific. Mar. Ecol. Prog. Ser. 375, 53–64.
Van Engeland, T., Soetaert, K., Knuijt, A., Laane, R., Middelburg, J., 2010. Dissolved organic nitrogen dynamics in the North Sea: A time series analysis (1995–2005). Estuar. Coast. Shelf Sci. 89, 31–42.
García-Martín, E.E., Daniels, C.J., Davidson, K., Davis, C.E., Mahaffey, C., Mayers, K.M.J., McNeil, S., Poulton, A.J., Purdie, D.A., Tarran, G., Robinson, C., this issue. Seasonal changes in microplankton respiration and bacterial metabolism in a temperate Shelf Sea. Progr. Oceanogr.
Giering, S., Wells, S., Mayers, K., Preece, C., Schuster, H., Cornwell, L., Fileman, E., Atkinson, A., Cook, K., Mayor, D., this issue. Mesozooplankton in the Celtic Sea: biomass and trophic position. Progr. Oceanogr.
Harrison, J.A., Caraco, N., Seitzinger, S.P., 2005. Global patterns and sources of dissolved organic matter export to the coastal zone: results from a spatially explicit, global model. Global Biogeochem. Cyc. 19. http://dx.doi.org/10.1029/2005GBC002480.
Hedges, J.I., 1992. Global biogeochemical cycles: progress and problems. Mar. Chem. 39, 67–93.
Hedges, J.I., Baldock, J.A., Gelinas, Y., Lee, C., Petereson, M., Wakeham, S.G., 2001. Evidence for non-selective preservation of organic matter in sinking marine particles. Nature 409, 801–804. http://dx.doi.org/10.1038/35057247.
Hedges, J.I., Baldock, J.A., Gelinas, Y., Lee, C., Peterson, M.L., Wakeham, S.G., 2002. The biochemical and elemental compositions of marine plankton: a NMR perspective. Mar. Chem. 78, 47–63.
Hopkinson, C.S., Fry, B., Nolin, A.L., 1997. Stoichiometry of dissolved organic matter dynamics on the continental shelf of the northeastern U.S.A. Cont. Shelf Res. 17 (5), 473–489.
Hopkinson, C.S., Vallino, J., 2005. Efficient export of carbon to the deep ocean through dissolved organic matter. Nature 433, 142–145. http://dx.doi.org/10.1038/nature03191.
Hydes, D., Aoyama, M., Aminot, A., Bakker, K., Becker, S., Coverly, S., Daniel, A., Dickson, A., Grosso, O., Keroul, R., van Ooijen, J., Sato, K., Tanhau, T., Woodward, E., Zhang, J.Z., 2010. Determination of dissolved nutrients (N, P, Si) in seawater with high precision and inter-comparability using gas-segmented continuous flow analysers. In: The GO-SHIP Repeat Hydrography Manual: A Collection of Expert Reports and Guidelines, IOCCP Report No. 14, ICPO Publications Series No. 134.
Humphreys, M.P., Achterberg, E.P., Chowdhury, M.Z.H., Griffiths, A.M., Hartman, S.E., Hopkins, J., Hull, T., Kivimäe, C., Smilenova, A., Wihsgott, J., Woodward, E.M.S., Moore, C.M., this issue. Mechanisms for a nutrient-conserving carbon pump in a seasonally stratified, temperate continental shelf sea. Prog. Oceanogr.
Jiao, N., Herndl, G.J., Hansell, D.A., Benner, R., Kattner, G., Wilhelm, S.W., Kirchman, D.L., Weinbauer, M.G., Luo, T., Chen, F., Azam, F., 2010. Microbial production of recalcitrant dissolved organic matter: long-term carbon storage in the global ocean. Nat. Rev. Microbiol. 8, 593–599. http://dx.doi.org/10.1038/nrmicro2386.
Johnson, M., Greenwood, N., Sivyer, D., Thomson, M., Reeve, A., Weston, K., Jickells, T., 2013. Characterising the seasonal cycle of dissolved organic nitrogen using Cefas SmartBuoy high-resolution time-series samples from the southern North Sea. Biogeochemistry 113, 23–36.
Kähler, P., Koeve, W., 2001. Marine dissolved organic matter: Can its C: N ratio explain carbon overconsumption? Deep Sea Res., Part I 48, 49–62.
Karl, D.M., Björkman, K.M., Dore, J.E., Fujieki, L., Hebel, D.V., Houlihan, T., Letelier, R.M., Tupas, L.M., 2001. Ecological nitrogen-tophosphorus stoichiometry at station ALOHA. Deep Sea Res Part II 48, 1529–1566.
Karl, D.M., Tien, G., 1992. MAGIC: A sensitive and precise method for measuring dissolved phosphorus in aquatic environments. Limnol. Oceanogr. 37, 105–116. http://dx.doi.org/10.4319/lo.1992.37.1.0105.
Kepkay, P.E., 1994. Particle aggregation and the biological reactivity of colloids. Mar. Ecol. Prog. Ser. 109, 293–304.
Klausmeier, C.A., Litchman, E., Daufresne, T., Levin, S.A., 2008. Phytoplankton stoichiometry. Ecol. Res. 23, 479–485. http://dx.doi.org/10.1007/s11284-008-0470-8.
Kolowith, L.C., Ingall, E.D., Benner, R., 2001. Composition and cycling of marine organic phosphorus. Limnol. Oceanogr. 46 (2), 309–320.
Lomas, M.W., Burke, A.L., Lomas, D.A., Bell, D.W., Shen, C., Dyhrman, S.T., Ammerman, J.W., 2010. Sargasso Sea phosphorus biogeochemistry: an important role for dissolved organic phosphorus (DOP). Biogeosciences 7, 695–710. http://dx.doi.org/10.5194/bg-7-695-2010.
Lønborg, C., Alvarez-Salgado, X., 2012. Recycling versus export of bioavailable dissolved organic matter in the coastal ocean and efficiency of the continental shelf pump. Global Biogeochem. Cycles 26, GB3018. http://dx.doi.org/10.1029/2012GB004353.
Mahaffey, C., Reynolds, S., Davis, C.E., Lohan, M.C., 2014. Alkaline phosphatase activity in the subtropical ocean: Insights from nutrient, dust and trace metal addition experiments. Front. Mar. Sci. 1, 1–13. http://dx.doi.org/10.3389/fmars.2014.00073.
Middelburg, J.J., Duarte, C.M., Gattuso, J.-P., 2004. Respiration in coastal benthic communities. In: del Giorgio, P.A., Williams, P.J.le B. (Eds.), Respiration in Aquatic Ecosystems. Oxford Univ. Press.
Moore, C.M., Sugget, D.J., Hickman, A.E., Kim, Y.-N., Tweddle, J.F., Sharples, J., Geider, R.J., Holligan, P.M., 2006. Phytoplankton photoacclimation and photoadaptation in response to environmental gradients in a shelf sea. Limnol. Oceanogr. 51 (2), 936–949.
Moran, M.A., Zepp, R.G., 1997. Role of photoreactions in the formation of biologically labile compounds from dissolved organic matter. Limnol. Oceanogr. 42 (6), 1307–1316.
Moschonas, G., Gowen, R., Stewart, B., Davidson, K., 2015. Nitrogen dynamics in the Irish Sea and adjacent shelf waters: An exploration of dissolved organic nitrogen. Estuar. Coast. Shelf Sci. 164, 276–287.
Murphy, J., Riley, J.P., 1962. A modified single solution method for the determination of phosphate in natural waters. Anal. Chim. Acta 27, 31–36.
Ogawa, H., Tanoue, E., 2003. Dissolved organic matter in oceanic waters. Journal of Oceanogr. 59 (2), 129–147.
Pemberton, K., Rees, A.P., Miller, P.I., Raine, R., Joint, I., 2004. The influence of water body characteristics on phytoplankton diversity and production in the Celtic Sea. Cont. Shelf Res. 24 (17), 2011–2028.
Plum, C., Hüsener, M., Hillebrand, H., 2015. Multiple vs. single phytoplankton species alter stoichiometry of trophic interaction with zooplankton. Ecology 96 (11), 3075–3089.
Popendorf, K., Duhamel, S., 2015. Variable phosphorus uptake rates and allocation across microbial groups in the oligotrophic Gulf of Mexico. Environ. Microbiol. 17, 3992–4006.
Poulton, A. J., Davis, C. E., Daniels, C. J., Mayers, K., Harris, C., Tarran, G. A., Widdicombe, C. E., and E. M. S. Woodward (this issue), Seasonal phosphorus dynamics in a temperate shelf sea (Celtic Sea): uptake, release, turnover and stoichiometry, Prog. Oceanogr.
Redfield, A.C., Ketchum, B.H., Richards, F.A., 1963. The Influence of Organisms on the Composition of Sea-water. In: Hill, M.N. (Ed.), The Sea. Wiley, New York, pp. 26–77.
Riley, J.S., Sanders, R., Marsay, C., Le Moigne, F.A.C., Achterberg, E.P., Poulton, A.J., 2012. The relative contribution of fast and slow sinking particles to ocean carbon export. Glob Biogeochem. Cycles 26, 1–10. http://dx.doi.org/10.1029/2011GB004085.
Miller, J.N., Miller, J.C., 2005. Statistics and Chemometrics for Analytical Chemistry, fifth ed. Pearson Education Ltd, London.
Simpson, J.H., Sharples, J., 2012. Introduction to the physical and biologicaloceanography of shelf seas. Cambridge University Press.
Sterner, R.W., Elser, J.J., 2002. Ecological Stoichiometry: The Biology of Elements from Molecules to the Biosphere. Princeton Univ. Press.
Thomas, H., Bozec, Y., Elkalay, K., de Baar, H.J.W., 2004. Enhanced open ocean storage of CO_2 from shelf sea pumping. Science 304, 1005–1008. http://dx.doi.org/10.1126/science.1095491.
Toggweiler, J., 1993. Carbon overconsumption. Nature 363, 210–211.
Tsunogai, S., Watanabe, S., Sato, T.T., 1999. Is there a “continental shelf pump” for the absorption of atmospheric CO_2? Tellus 51B, 701–712.
Wihsgott, J., Sharples, J., Hopkins, J., Woodward, E., Greenwood, N., Hull, T., Sivyer, D., this issue. Investigating the autumn bloom’s significance within the seasonal cycle of primary production in a temperate shelf sea. Prog. Oceanogr.
Williams, C.A., Sharples, J., Mahaffey, C., Rippeth, T., 2013. Wind-driven nutrient pulses to the subsurface chlorophyll maximum in seasonally stratified shelf seas. Geophys. Res. Lett. 40, 5467–5472. http://dx.doi.org/10.1002/2013GL058171.
Wilson, J.M., Severson, R., Beman, J.M., 2014. Ocean-scale patterns in community respiration rates along continuous transects across the Pacific Ocean. PLOS ONE. http://dx.doi.org/10.371/journal.pone.0099821.
Wollast, R., 1998. Evaluation and comparison of the global carbon cycle in the coastal zone and in the open ocean. In: In: Brink, K.H., Robinson, A.R. (Eds.), The Sea, vol. 10. John Wiley, New York, pp. 213–252.
Woodward, E.M.S., Rees, A.P., 2001. Nutrient distributions in an anticyclonic eddy in the North East Atlantic Ocean, with reference to nanomolar ammonium concentrations. Deep-Sea Res. II 48, 775–794.
Yamamuro, M., Kayanne, H., 1995. Rapid direct determination of organic-carbon and nitrogen in carbonate-bearing sediments with a yanaco mt-5 chn analyzer. Limnol. Oceanogr. 40, 1001–1005.